materials proceedings

MDPI

Proceeding Paper

Development of a Process for Low-Cost LFP Batteries Treatment †

Rafaella-Aikaterini Megaloudi, Alexandros Galanis, Paschalis Oustadakis and Anthimos Xenidis *

School of Mining and Metallurgical Engineering NTUA, 157 72 Zografou, Greece; megaloudik@mail.ntua.gr (R.-A.M.); alexandrosgalanes@gmail.com (A.G.); oustadak@metal.ntua.gr (P.O.)

* Correspondence: axen@metal.ntua.gr

† Presented at the 2nd International Conference on Raw Materials and Circular Economy "RawMat2023", Athens, Greece, 28 August–2 September 2023.

Abstract: The recycling of lithium iron phosphate ($LiFePO_4$) batteries from electric and hybrid vehicles was investigated, by applying mechanical pretreatment and hydrometallurgical methods. The aim was to extract lithium (Li) into the aqueous solution and precipitate iron (Fe) in the form of ferric iron phosphate ($FePO_4$). Samples of lithium iron phosphate (LFP) batteries from small electric vehicles provided by the company BEEV were used in this study. Initially, the black mass was isolated using mechanical crushing, screening, and sink–float separation methods, avoiding the need for costly chemical or thermal treatments. The cathodic material was then leached with sulfuric acid (H_2SO_4) and hydrogen peroxide (H_2O_2) to oxidize ferrous to ferric iron, resulting in the precipitation of iron phosphate, which was collected in the solid residue from the leaching process. Leaching tests were conducted by varying the concentrations of sulfuric acid and hydrogen peroxide, as well as the leaching time. It has been indicated that by using a sulfuric acid concentration equal to the stoichiometric requirement, and hydrogen peroxide at four times the stoichiometric amount, Li extraction of greater than 98% was achieved within the first few minutes of leaching, while iron extraction remained below 0.5%.

Keywords: LFP batteries; leaching; sulfuric acid; hydrogen peroxide

check for updates

Citation: Megaloudi, R.-A.; Galanis, A.; Oustadakis, P.; Xenidis, A. Development of a Process for Low-Cost LFP Batteries Treatment. *Mater. Proc.* **2023**, *15*, 96. https://doi.org/10.3390/materproc2023015096

Academic Editors: Antonios Peppas, Christos Roumpos and Charalampos Vasilatos

Published: 25 March 2025

Copyright: © 2025 by the authors. Licensee MDPI, Basel, Switzerland. This article is an open access article distributed under the terms and conditions of the Creative Commons Attribution (CC BY) license (https://creativecommons.org/licenses/by/4.0/).

1. Introduction

The European Commission's announcement of the European Green Deal in December 2019 represents a strategic plan to guide the European Union's transition towards a climate-neutral economy. This includes a commitment to reduce carbon emissions by 55% by 2030 and achieve carbon neutrality by 2050 [1]. A shift away from fossil fuels and a growing electric vehicle market are influencing the automotive industry. Embracing electrification is a logical outcome of this trend. As a result, the production of batteries is increasing, emphasizing the critical need for advancements in recycling technologies.

Electric vehicle batteries contain critical raw materials such as lithium (Li), nickel (Ni), cobalt (Co), graphite, and phosphorus (P), which are economically important for the EU but also present a high supply risk [2]. The average annual price of lithium carbonate in long-term contracts has more than doubled since 2020, reaching EUR 17,000 per ton in 2021. Spot prices have shown even greater volatility, rising from approximately EUR 5500 per ton in September 2020 to over EUR 76,000 per ton in September 2022 [3]. Looking ahead, by around 2025, lithium carbonate prices could potentially decline to EUR 10,000 per ton [4].

Among the battery technologies available for electric vehicles (EVs), Li-ion batteries stand out as the most promising option and are currently regarded as the most suitable choice for advancing the development of the next generation of EVs [5–7]. Lithium iron phosphate ($LiFePO_4$) batteries possess several advantages that distinguish them among various types of lithium-ion batteries. These advantages include their special safety features, long lifespan, cost-effectiveness, good thermal stability, and environmental friendliness (being non-toxic and recyclable) [5,8].

The efficient and cost-effective recycling of valuable components from LFP batteries can be achieved through hydrometallurgical methods. These methods involve the extraction of lithium from the battery's black mass (comprising the cathode and anode materials) using sulfuric acid and hydrogen peroxide as an oxidizing agent, which converts ferrous to ferric iron, resulting in its precipitation as ferric phosphate. Additionally, impurities such as iron (Fe), copper (Cu), and aluminum (Al) in the pregnant leach solution are separated as hydroxides, and the process culminates in the recovery of lithium as lithium carbonate [9–13].

In this study, parameters affecting the recycling of LFP batteries from electric and hybrid vehicles by leaching with sulphuric acid and hydrogen peroxide solutions at various concentrations aiming at Li recovery in solution and the precipitation of iron as iron phosphate were investigated.

2. Materials and Methods

Twelve fully discharged, spent LFP battery cells, sourced from the company BEEV (Beev, Bauer Energy, Glyka Nera, Attica, Greece), were used. Initially, the battery cells were opened and crushed using an Alligator Shearing Machine (Radhe Krishna Hydro Tech, Gurgaon, Gurugram—Haryana, India). Then, an SM 2000 Heavy-Duty Cutting Mill (F. Kurt Retsch GmbH and Co KG, Haan, Germany) was used for shredding and simultaneous grinding to a particle size of 3.15 mm, without prior manual separation.

After drying the sample at 100 °C to remove any remaining electrolyte, particle size distribution analysis was performed by dry sieving with an RX-29 RO-TAP Sieve Shaker (W.S. Tyler, OH, USA). Plastics were then effectively removed from the −3.15 mm fraction through sink–float separation using water as the medium. The remaining material was re-dried and further ground to −160 μm using a Model LM2 Laboratory Pulverizer (Labtechnics, Phillips Ormonde Fitzpatrick, Vic 3000, Australia), producing the working sample.

Chemical analysis of the black mass sample thus produced was carried out following fusion with borax and measurement of elements in the solution derived by ICP-OES (Optima 7000, PerkinElmer, Akron, OH, USA) and atomic absorption spectroscopy (AAS) (PinAAcle 900T, PerkinElmer, Akron, OH, USA). For fusion, 0.1 g of the black mass sample was mixed with 1.5 g of a mixture of potassium carbonate, sodium carbonate, and sodium tetraborate decahydrate at a 1:1:1 molar ratio. This mixture was further heated in a platinum crucible at 1000 °C for 1 h.

The carbon content in the solid material was analyzed using a LECO furnace analyzer (LECO Middle East International FZE, Dubai, UAE). X-ray diffraction (XRD) patterns were obtained using a MiniFlex 600 benchtop diffractometer (Rigaku, Tokyo, Japan), equipped with a D/tex Ultra detector and operated at 40 kV and 15 mA (600 W) with Cu-Kα radiation. Diffraction data were collected over a 2θ range of 5–80°, with 0.02° increments and a scan rate of 5° per minute. Phase identification was performed using Crystallographica Search–Match v2.1.1.1 software.

Leaching tests were performed using sulfuric acid (H_2SO_4, 98%, Sigma Aldrich, St. Louis, MO, YSA) and hydrogen peroxide (H_2O_2, 30%, Sigma Aldrich). The leaching experiments of the black mass were conducted in a 500 mL round-bottom glass reactor placed in a thermostatically controlled mantle, agitated at 400 rpm, and maintained at 60 °C. The reactor was equipped with a four-necked lid, with a thermocouple inserted in one of the openings to continuously monitor the temperature and a condenser for vapor cooling.

The pH of the resulting leachates was determined using a Metrohm 913 laboratory pH meter equipped with a Porotrode 3M KCl pH electrode. The redox potential was measured using a Metrohm silver/silver chloride (Ag/AgCl in saturated KCl) electrode.

Following the extraction tests, all necessary analyses were conducted on both the resulting leachate and the solid residues. Leachates were analyzed by ICP-OES and AAS to determine the Fe, Al, Cu, and Li concentration in solutions. Orthophosphate ions (PO_4^{3-}) in the samples were determined using pre-packaged reagent vials from Hach (Hach Lange

GmbH, Düsseldorf, Germany). These ions in the sample reacted with the molybdenum reagent to form a phosphomolybdenum complex. The addition of ascorbic acid to the reagent reduced the complex, resulting in the strong blue color of molybdenum, and the absorption was measured at 710 nm. Quantification was performed using a stored curve in the HACH DR 1900 spectrophotometer.

The solid residues from the leaching experiments were dissolved by fusion with borax, and the concentrations of Fe, Al, Cu, and Li in the emanating solution were determined by ICP-OES and AAS. The orthophosphate ions were quantified once again using the pre-packaged reagents from HACH and the pre-stored curve in the HACH DR 1900. Furthermore, mineralogical analysis was performed on the solid residues using X-ray diffraction (XRD).

3. Results and Discussion

3.1. Pretreatment

The total mass of the dry material obtained from crushing, cutting, and drying 12 spent cylindrical LFP-type battery cells was 1403.78 g. This material was then separated by screening using 3.15 mm and 160 µm mesh sizes into three distinct fractions: (a) the +3.15 mm fraction (6.7 g), consisting primarily of metals; (b) the −160 µm fraction (267.03 g), which contained mainly the active anodic and cathodic materials (black mass); and (c) the intermediate fraction (−3.15 mm +160 µm), which contained remaining metals, plastics, and black mass. This intermediate fraction was further subjected to sink-and-float separation using water to remove plastics (58.47 g), followed by a second stage of drying, grinding, and sieving, which produced a coarse (+160 µm) fraction containing metals and some remaining plastics (567.79 g) and a fine (−160 µm) black mass fraction, which was then combined with the black mass collected from the first stage of crushing and grinding, resulting in a total mass of 770.82 g, corresponding to 54.91% of the initial mass of the LFP batteries.

3.2. Sample Characterization

The results of chemical and mineralogical analysis of the black mass are given in the following Table 1 and Figure 1.

As is indicated in Table 1, the LFP battery sample is primarily composed of C (40%), PO_4^{3-}; (32.32%), Fe (20.57%), Li (2.49%), Al (1.87%), and Cu (0.87%). The content of the three primary constituents of the cathodic LFP material, i.e., Li, Fe, and PO_4^{3-}, in black mass is 0.368, 0.359, and 0.340 moles/100 g, respectively, corresponding to molar ratios approximately equal to 1:1:1, which are characteristic of the $LiFePO_4$ cathodic material.

The concentrations of the three primary constituents of the cathodic LFP material—Li, Fe, and PO_4^{3-}—in the black mass are 0.368, 0.359, and 0.340 moles per 100 g, respectively.

As is indicated in Figure 1, the main mineralogical phases identified from the XRD pattern of the black mass are and triphylite ($LiFePO_4$ – Green in the 1st diagram), graphite (C, blue), metallic copper (Cu, light blue), and aluminum (Al, light brown).

Table 1. Chemical analysis of LFP black mass.

Element/Ion	Content (%)	Content (Moles/100 g)
Fe	20.57	0.368
Li	2.49	0.359
PO_4^{3-}	32.32	0.340
Al	1.87	0.069
Cu	0.87	0.014
C	40	3.333

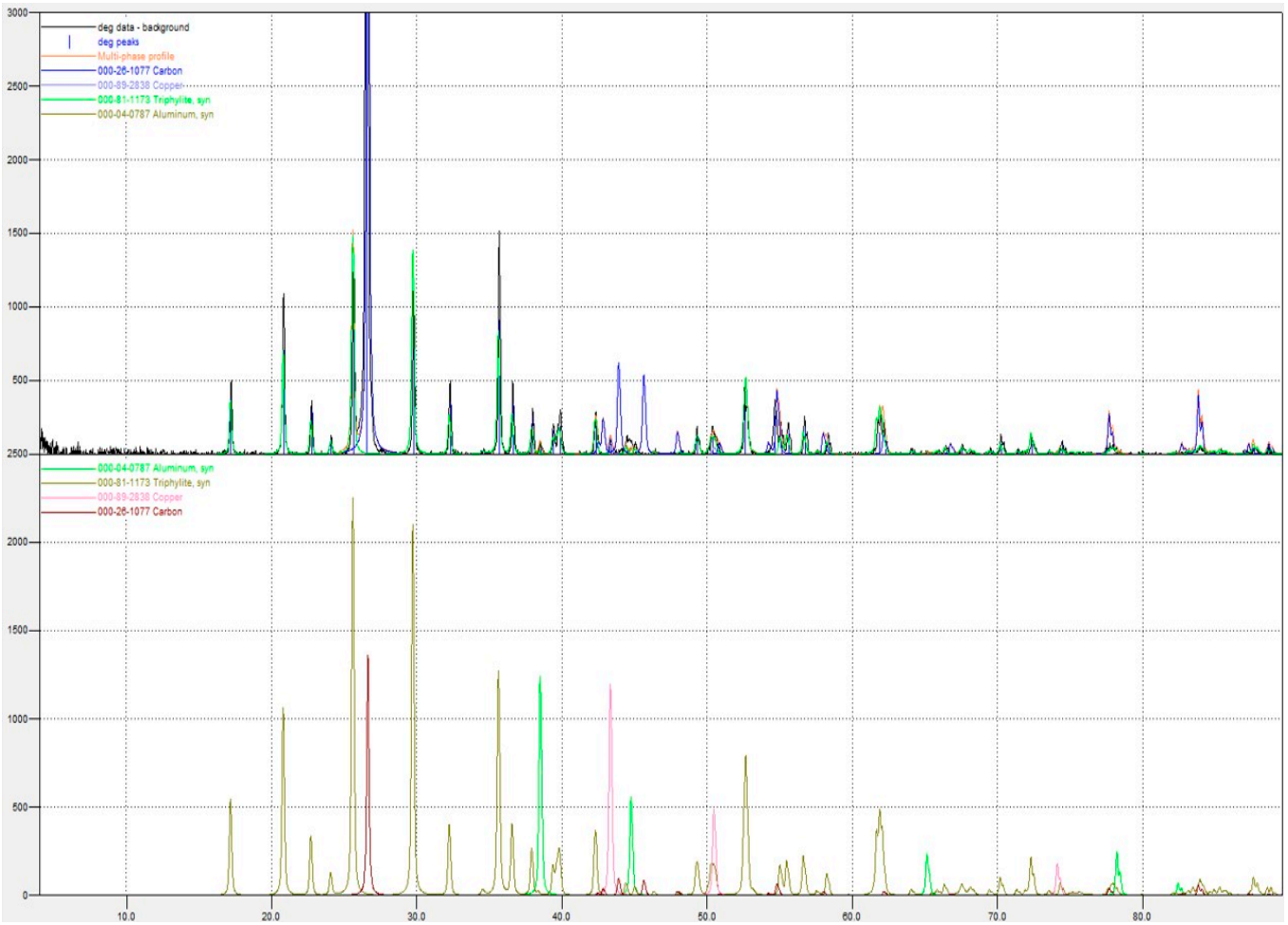


Figure 1. XRD pattern of the black mass sample.

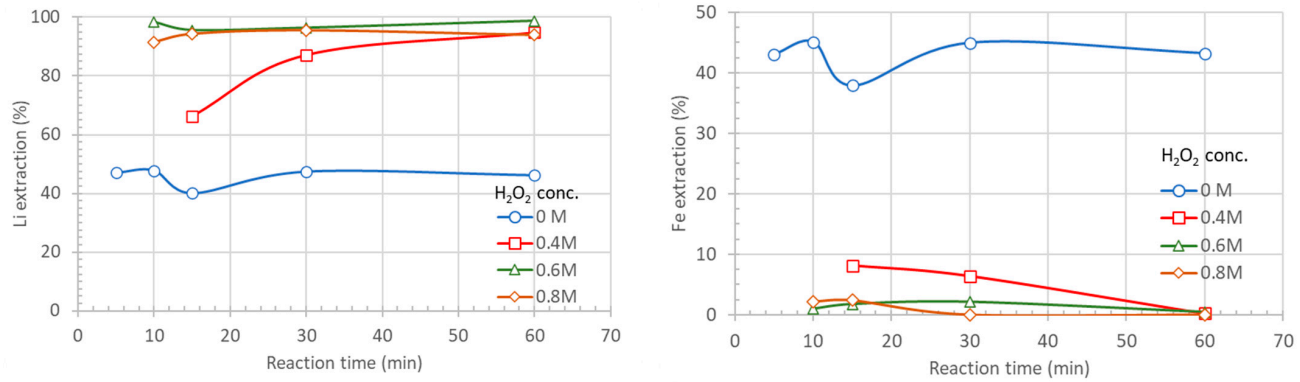
3.3. Leaching Tests

Based on the chemical analysis of the black mass, the stoichiometric quantities of sulfuric acid and hydrogen peroxide were calculated to be 0.18 M, assuming the leaching process was conducted at a liquid-to-solid ratio of 10 L/kg. Consequently, leaching experiments were performed using 0.2, 0.25, and 0.3 M sulfuric acid, as well as 0, 0.4, 0.6, and 0.8 M hydrogen peroxide, to investigate the extraction of lithium, iron, aluminum, and copper.

In the following figures the results of lithium (Figure 2a) and iron (Figure 2b) extraction vs. hydrogen peroxide concentration and time, at a 0.2 M sulfuric acid concentration, are presented.

As is shown in Figure 2a, lithium extraction reaches nearly 100% when the H_2O_2 concentration exceeds 0.6 M. Under the same conditions, iron extraction remains very low, below 0.5%, suggesting that under these pH and redox conditions, it is predominantly oxidized to Fe(III) and precipitated as ferric iron phosphate (Figure 2b). At an H_2O_2 concentration of 0.4 M, the kinetics of lithium dissolution and ferric iron precipitation are slower; however, nearly 100% lithium extraction and 0% iron extraction are achieved after a residence time of 1 h.

At sulfuric acid concentrations higher than 0.2 M, iron and phosphates are leached into the solution, and even at a hydrogen peroxide concentration of 0.8 M, their extraction into the leachate remains significant (6.1% and 2.1%, respectively). The best leaching results, in terms of lithium, iron, and phosphate extraction, were obtained using a leaching solution of 0.2 M H_2SO_4; and 0.6 M H_2O_2. Detailed extraction results for all elements investigated under these leaching conditions are presented in Figure 3.



(**a**) (**b**)

Figure 2. Extraction of (**a**) Li and (**b**) Fe vs. time and H_2O_2 concentration in the leaching solution (H_2SO_4 conc 0.2 M).

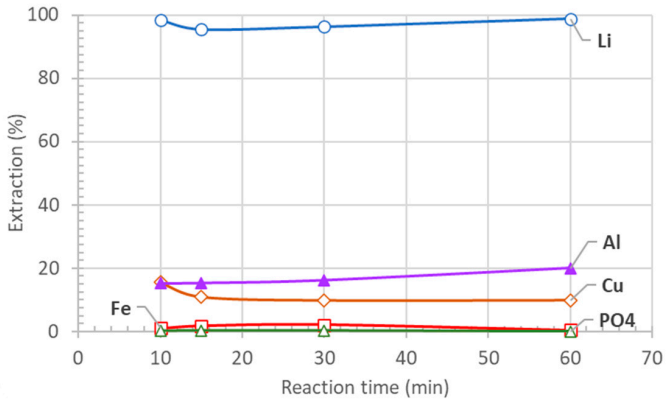


Figure 3. Extraction of Li, Fe, PO4, Cu, and Al vs. time (0.2 M H_2SO_4 and 0.6 M H_2O_2 concentrations).

As is shown in Figure 3, after a residence time of one hour, 98.8% of lithium, 9.92% of copper, and 20.02% of aluminum are extracted into the leaching solution, whereas iron and phosphates remain in the solid residue with extraction rates below 0.5% and 0.05%, respectively. Under the applied experimental conditions, the kinetics of lithium dissolution and iron precipitation are rapid, reaching their maximum values within the first few minutes.

3.4. Mineralogical Analysis of Solid Leach Residue

The XRD pattern of the solid residue from black mass leaching with 0.2 M H_2SO_4 and 0.6 M H_2O_2 solutions, compared to the untreated black mass sample, is shown in Figure 4.

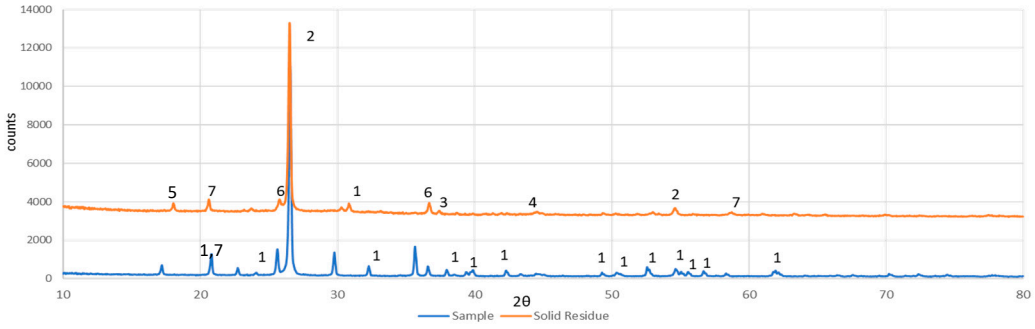


Figure 4. XRD patterns of solid residue (brown line) (leaching with 0.2 M H_2SO_4 and 0.6 M H_2O_2 solutions for one hour) as compared with the initial black mass (blue line) sample (1 $LiFePO_4$, 2 Graphite, 3 Al, 4 Cu, 5 PVDF, 6 $FePO_4$, 7 $AlPO_4$ (Berlinite)).

Figure 4 shows that the peaks corresponding to $LiFePO_4$ have disappeared and been replaced by peaks of $FePO_4$ and $AlPO_4$, indicating that lithium has dissolved while iron has precipitated as iron phosphate. The binder remains detectable in the solid leach residue, suggesting that its decomposition is not essential for successful leaching [10].

4. Conclusions

In this study, battery cells were processed without prior manual sorting and were treated primarily using mechanical processes, avoiding the need for expensive chemical or thermal methods to isolate the cathode and anode materials and prepare them for leaching. The black mass (<160 μm) obtained from mechanical pretreatment accounted for 55% of the battery cell sample. Using a sulfuric acid concentration of 0.2 M and a hydrogen peroxide concentration of 0.6 M, nearly complete lithium extraction into the aqueous phase (>95–100%) was achieved, along with negligible iron extraction (precipitated as iron phosphate in the solid residue) and minor extraction of aluminum and copper. The leaching reactions were rapid, and successful extractions were accomplished without binder decomposition.

Author Contributions: Conceptualization, A.X. and P.O.; methodology, P.O. and R.-A.M.; validation, R.-A.M. and A.G.; investigation, R.-A.M. and A.G.; writing—original draft preparation, R.-A.M.; writing—review and editing, R.-A.M. and A.X.; supervision, A.X.; project administration, A.X.; funding acquisition, A.X. All authors have read and agreed to the published version of the manuscript.

Funding: This research was funded by the Basic Research Program PEVE 2020 of the National Technical University of Athens.

Institutional Review Board Statement: Not applicable.

Informed Consent Statement: Not applicable.

Data Availability Statement: Data sharing is not applicable to this article.

Acknowledgments: The authors acknowledge the company Bauer Energy, Glyka Nera, Attica, Greece, for providing LFP batteries.

Conflicts of Interest: The authors declare no conflict of interest.

References

1. Sikora, A. European Green Deal—Legal and financial challenges of the climate change. *ERA Forum* **2021**, *21*, 681–697. [CrossRef]
2. European Commission, Directorate-General for Internal Market, Industry, Entrepreneurship and SMEs; Grohol, M.; Veeh, C. Study on the Critical Raw Materials for the EU 2023—Final Report, Publications Office of the European Union. 2023. Available online: https://data.europa.eu/doi/10.2873/725585 (accessed on 20 November 2024).
3. U.S. Geological Survey. Mineral Commodity Summaries 2022. (October 2023). Available online: http://pubs.er.usgs.gov/publication/mcs2022 (accessed on 20 November 2024).
4. Sun, X.; Ouyang, M.; Hao, H. Surging lithium price will not impede the electric vehicle boom. *Joule* **2022**, *6*, 1738–1742.
5. Chen, X.; Shen, W.; Vo, T.T.; Cao, Z.; Kapoor, A. An overview of lithium-ion batteries for electric vehicles. In Proceedings of the 10th International Power & Energy Conference (IPEC), Ho Chi Minh City, Vietnam, 12–14 December 2012; pp. 230–235. [CrossRef]
6. Camargos, P.H.; dos Santos, P.H.J.; dos Santos, I.R.; Ribeiro, G.S.; Caetano, R.E. Perspectives on Li-ion battery categories for electric vehicle applications: A review of state of the art. *Int. J. Energy Res.* **2022**, *46*, 19258–19268. [CrossRef]
7. Fan, E.; Li, L.; Wang, Z.; Lin, J.; Huang, Y.; Yao, Y.; Chen, R.; Wu, F. Sustainable recycling technology for Li-Ion batteries and beyond: Challenges and future prospects. *Chem. Rev.* **2020**, *120*, 7020–7063. [CrossRef] [PubMed]
8. Hannan, M.A.; Hoque, M.M.; Hussain, A.; Yusof, Y.; Ker, P.J. State-of-the-Art and energy management system of lithium-ion batteries in electric vehicle applications: Issues and recommendations. *IEEE Access* **2018**, *6*, 19362–19378. [CrossRef]
9. Wang, M.; Liu, K.; Dutta, S.; Alessi, D.S.; Rinklebe, J.; Kim, K. Recycling of lithium iron phosphate batteries: Status, technologies, challenges, and prospects. *Renew. Sustain. Energy Rev.* **2022**, *163*, 112515. [CrossRef]
10. Larouche, F.; Tedjar, F.; Amouzegar, K.; Houlachi, G.; Bouchard, P.; Demopoulos, G.P.; Zaghib, K. Progress and status of hydrometallurgical and direct recycling of Li-Ion batteries and beyond. *Materials* **2020**, *13*, 801. [CrossRef] [PubMed]
11. Li, H.; Xing, S.; Liu, Y.; Li, F.; Guo, H.; Kuang, G. Recovery of Lithium, Iron, and Phosphorus from Spent $LiFePO_4$ Batteries Using Stoichiometric Sulfuric Acid Leaching System. *ACS Sustain. Chem. Eng.* **2017**, *5*, 8017–8024. [CrossRef]

12. Kumar, J.; Neiber, R.R.; Park, J.; Soomro, R.A.; Greene, G.W.; Mazari, S.A.; Seo, H.Y.; Lee, J.Y.; Shon, M.; Chang, D.W.; et al. Recent progress in sustainable recycling of $LiFePO_4$-type lithium-ion batteries: Strategies for highly selective lithium recovery. *Chem. Eng. J.* **2022**, *431*, 133993. [CrossRef]
13. Eronen, J.E.K. Recovery of Lithium from Lithium-Ion Battery Waste. Master Thesis, Aalto University: The Department of Chemical and Metallurgical Engineering, Espoo, Finland, 2017; 112p. Available online: https://aaltodoc.aalto.fi/bitstream/handle/123456789/27037/master_Eronen_Emmi_2017.pdf?sequence=1&isAllowed=y (accessed on 20 November 2024).

Disclaimer/Publisher's Note: The statements, opinions and data contained in all publications are solely those of the individual author(s) and contributor(s) and not of MDPI and/or the editor(s). MDPI and/or the editor(s) disclaim responsibility for any injury to people or property resulting from any ideas, methods, instructions or products referred to in the content.